Impact of Stator Segmentation on the Performance of Aerospace Propulsion Machines

R. M. Ram Kumar [1] **, Gaurang Vakil** [1] **, David Gerada** [1] **, Chris Gerada** [1] **, James Minshull** [2]

[1] Power Electronics, Machines and Control Group, University of Nottingham, Nottingham NG7 2RD, U.K

[2] Aerospace Technology Institute, Cranfield, MK43 OTR, U.K

Abstract

Electric machines offering a high power density are required for aerospace applications. Soft magnetic material with a high saturation flux density is one of the key component which is required to realize these power density targets. The need for a high saturation flux density necessitates the use of cobalt iron lamination over the conventional silicon steel. However, cobalt iron is very expensive i.e. order of 10 in comparison to silicon steel. Stator segmentation is identified as an appropriate method to reduce the wastage and cost associated with lamination. Consequently, in this paper, stator segmentation is analyzed on a 1.35 MW, 16-pole 48-slot propulsion machine. The impact of manufacturing is accounted by controlling the resulting airgap between the segmented structures. Electromagnetic performance for various segmented topologies are compared in terms of torque, torque ripple, and iron loss. Average torque is found to degrade by nearly 10% with an increase in the number of stator segments and the thickness of resulting airgap. Therefore, a tight tolerance is required between the segmented parts to retain the electromagnetic performance. On the other hand, this increases the cost of fabrication and nullifies the benefits offered by stator segmentation.

Introduction

Air transport is one is the least green forms of passenger transportation [1]. This has resulted in the development of several stringent technological roadmaps aimed at reducing the net carbon emissions. Hybrid-aircraft technology shown in Figure 1 is identified as a viable option to realize these strict pollution targets [2]. A fraction of the conventional fuel based propulsion is replaced with battery powered system in the hybrid aircraft. The electrified part of the hybrid-aircraft powertrain is represented in green in Figure 1. An electric machine is the heart of the electrified aircraft propulsion system.

Electric machines employed in aerospace applications are required to exhibit very high torque and power density [3]. Brushless DC and switched reluctance machine were favoured in the past due to their lightweight and increased reliability [4]. However, permanent magnet synchronous machine (PMSM) is gaining traction with the availability of advanced permanent magnet (PM) technologies [3]. Electric machines developed for various aerospace applications are listed in [5]. This covers electric machines ranging from few kWs up to few hundred kWs. PMSM with surface permanent magnet and Halbach array are found to be the invariable choices in these machines. The absence of rotor lamination in a Halbach rotor reduces its weight and contributes towards increased power density compared to surface mount PMSM. Sinusoidal airgap flux density, self-shielding effect and increased airgap flux density are few other advantages offered by Halbach PMSM

[6]. All the aforementioned advantages promote Halbach PMSM as a viable candidate for aerospace applications.
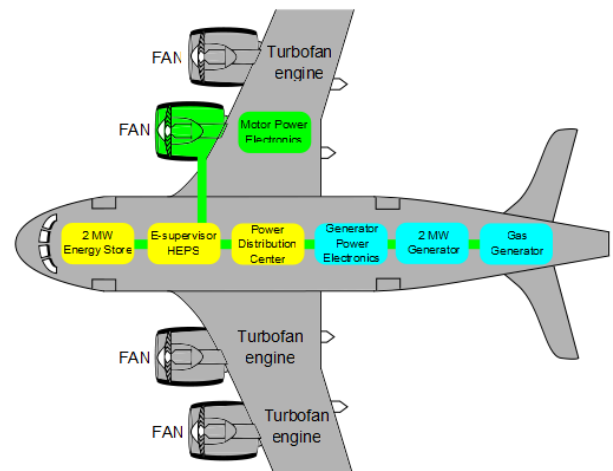
Soft magnetic material with a high saturation flux density i.e. cobalt-iron (CoFe) is required to realize the challenging power density targets of the aerospace industry [7]. The improvement in torque and power density of a Halbach machine which are achieved by using CoFe lamination are highlighted in [8]. The specific loss of CoFe is nearly same as the best available grade of silicon steel lamination [7]. The drawbacks of CoFe are its slightly higher mass density and significantly higher cost [9] in comparison to silicon steel. The offset presented by mass density is completely outweighed by its high saturation flux density. In contrast, it is possible to recover the high initial investment which is made on CoFe lamination only from the reduced running price. Consequently, it is essential to identify methods to decrease the requirement for expensive CoFe lamination.

Progressive punching is conventionally performed on electrical lamination to reduce its resulting wastage. This is suitable for electrical machines with rotors made of lamination like induction machine, interior permanent magnet machine, surface mount PMSM, wound field synchronous machine, synchronous reluctance machine and switched reluctance machine. On the other hand, the Halbach PMSM does not require rotor lamination. In addition, the high-power propulsion machines designed for aerospace applications have a bigger bore diameter

[10]. Therefore, cutting the stator as a single section will result in enormous wastage of lamination as shown in Figure 2. The useful section represents the stator section while the wastage refers to the remaining portion of the lamination. In this particular case, the useful section is only around 18% of the total area. Therefore, conventional method of stator fabrication will result in 82% waste of useful and expensive CoFe lamination.
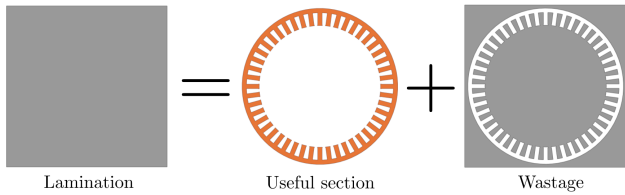
Figure 2: Wastage resulting from manufacturing stator as a single piece

Stator segmentation is identified as a potential method to reduce the wastage of lamination [11]. The impact of stator segmentation on cogging torque and torque ripple are analyzed in [12] and [13] respectively. The presence of gaps between stator segments is found to increase the magnitude of cogging torque [12]. These gaps are due to manufacturing limitations [12] and results in additional airgap seen by the electric machine. Therefore, these airgaps are expected to impact the average torque produced by a segmented electric machine. Consequently, it becomes essential to analyze the degradation in average torque resulting from stator segmentation. The different methods of stator segmentation are shown in Figure 3. Single tooth segmentation at the yoke and tooth-yoke interface are shown in Figures 3(a)nd 3(b) respectively. These types of segmentation are preferred for electric machine with concentrated winding. This enables easy automation of the winding process. On the other hand, the circumferential segmentation of the stator winding which is favoured for distributed winding is shown in Figure 3(c). Circumferential stator segmentation allows automation and easy insertion of winding over a pole-pair.
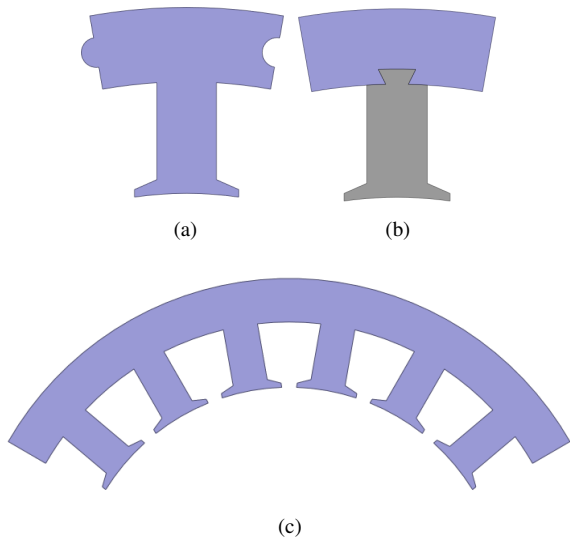
Figure 3: Topologies showing (a) single tooth segmentation at the yoke (b) single tooth segmentation at the tooth-yoke interface (c) circumferential segmentation for stator

Plug-in pole shoe is one other method of stator segmentation [11]. Plug-in pole shoe eases the manufacturing process but does not help increase the utilization of stator lamination. Therefore, only tooth and core segmented stators are selected for further studies. This paper is structured as follows. The benchmark design of a 1.35 MW , 16-pole 48-slot aerospace propulsion machine is given in the next section. This is followed by studying the impact of stator segmentation on the benchmark machine in the subsequent sections. The final section discusses the results and highlights the major outcomes of this paper.

Design of Benchmark Halbach Machine

Analyzing the impact of stator segmentation based on the utilization of lamination, average torque, torque ripple and iron loss is the main aim of this paper. Therefore, it is essential to benchmark all topologies of stator segmentation against the conventional single piece stator. The design and performance of Halbach PMSM with conventional single piece stator is elaborately discussed in this section. The benchmark Halbach PMSM is designed using the materials listed in Table 1. Power density is the main motivator behind the selection of materials listed in Table 1.

Table 1: Materials used in benchmark machine

Part	Material
Stator lamination	CoFe - 0.1 mm thickness
Permanent magnet	NdFeB - G48UH
Insulation	Class C - 220°
Housing	Aluminium
Shaft	Titanium

The superior saturation flux density of around 2.3 T obtained with CoFe lamination significantly supports towards weight savings. Samarium Cobalt (SmCo) magnets with a high continuous working temperature of 250 °C are preferred for high power density applications like aerospace and motorsport [14]. However, NdFeB magnets display a higher energy density compared to SmCo magnets and also displays an improved thermal stability with the addition of Dysprosium. Therefore, high energy density and high temperature withstanding G48UH grade NdFeB magnets are selected for this application.

16-pole and 48-slot configuration is selected based on the preliminary electromagnetic analysis. The Halbach array in the rotor is made of 5 pieces per pole as shown in Figure 4(a). The magnetization direction of various magnets in the Halbach array is shown in Figure 4(a). Semi-flooded oil jet cooling as shown in Figure 4(b) is used to limit the maximum operating temperature of the magnets and stator winding within the allowable limits. The PMs in the rotor of a high-speed Halbach PMSM is retained using a sleeve. The sleeve is usually made of non-magnetic material. The thickness of the sleeve adds to the airgap of the machine. This results in a significantly high airgap for high-speed halbach PMSM. The airgap harmonics content is relatively less due to this wide airgap. Therefore, the eddy current losses is a high-speed Halbach PMSM machine is reduced greatly. This eliminates the need for rotor cooling. Additionally, flooding the entire machine will result in significant drag induced losses at high-speed operations. Considering all this, a semi-flooded oil jet cooling is selected for this application.

A multi-domain sizing tool for Halbach machine is developed as shown in Figure 5 and used for obtaining an optimal propulsion machine. Multi Objective Genetic Algorithm (MOGA) based optimization is used for this process. The input variables, optimization core and output variables are shown in Figure 5. A valid design should achieve a power factor greater than 0.7 to avoid an oversized converter, and an efficiency greater than 95%. It should also have the continuous operating temperature within the allowable limits.

Table 2: Simulation results of benchmark Halbach PMSM

Parameter	Value
Average Torque (Nm)	651.34
Torque ripple (%)	6.16
Iron Loss (W)	5447.02

The optimal design is selected so to maximize the power density and its performance are given in Table 2. The optimal machine is found to

(a)   (b)
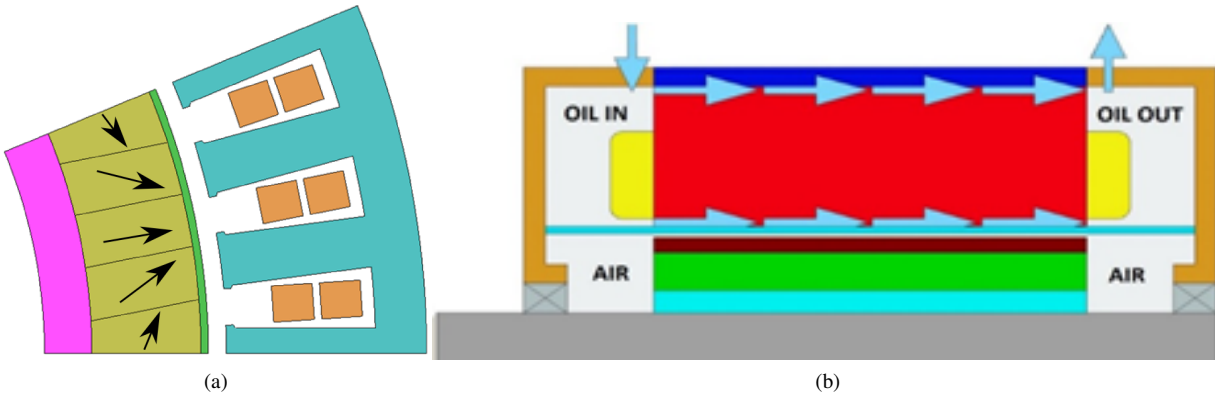
Figure 4: Benchmark Halbach PMSM showing (a) magnet orientation considering 5 pieces per pole (b) semi-flooded cooling
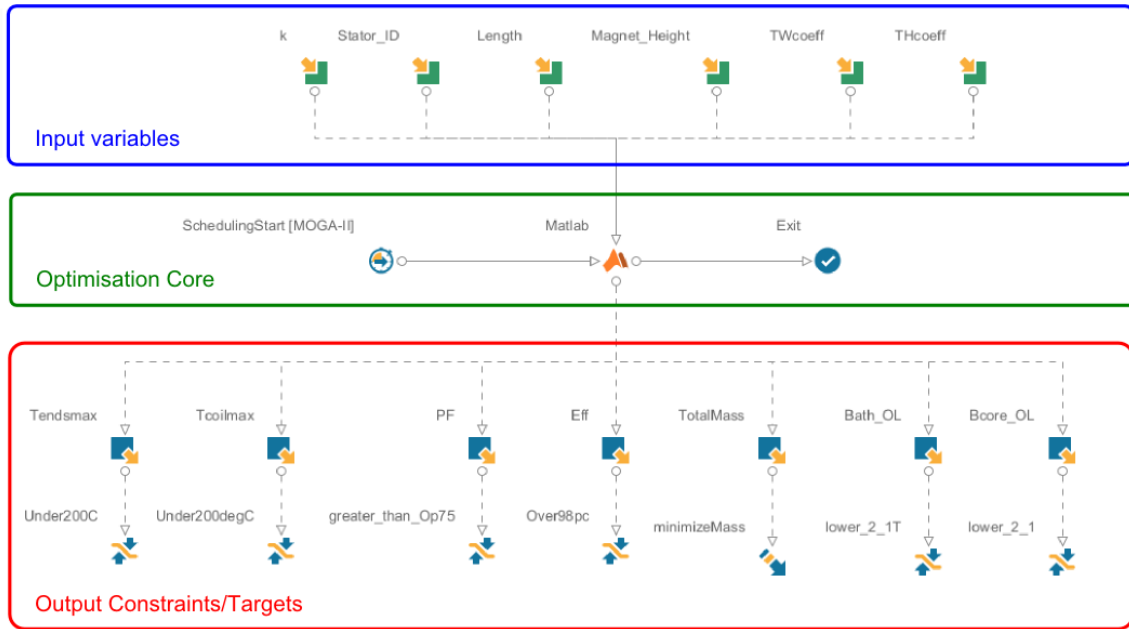
Figure 5: Layout of Halbach machine sizing tool

(a)   (b)
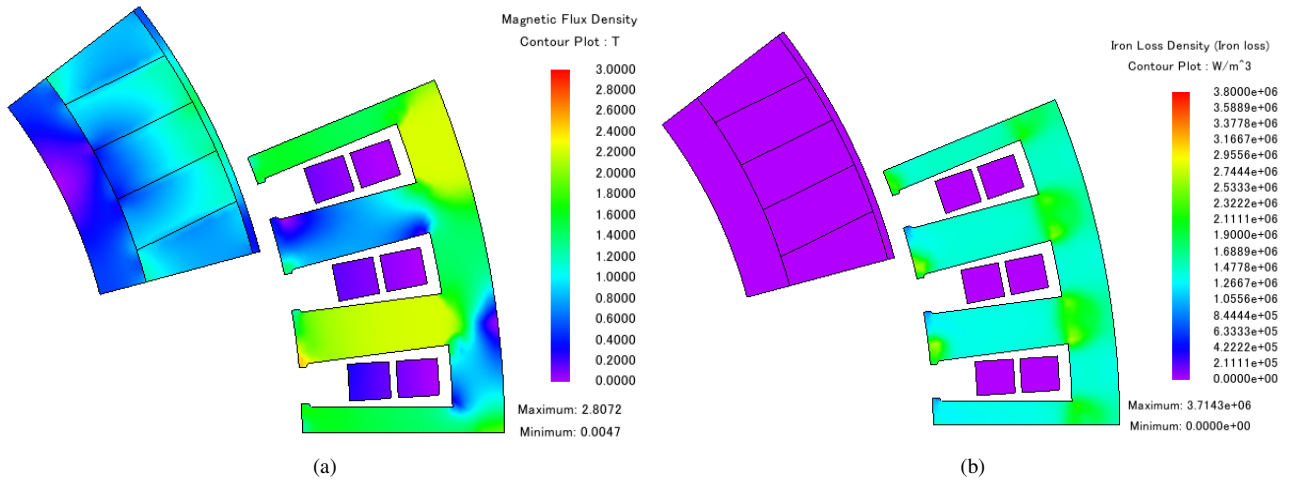
Figure 6: Simulation results at rated operating conditions for benchmark Halbach PMSM showing (a) flux density distribution (b) iron loss density

satisfy the specification of 1.35 MW. The iron loss is obtained by considering a build factor of 2. This accounts for an increase in iron loss resulting from manufacturing. Flux density distribution of the benchmark Halbach PMSM at rated operating conditions is shown in Figure 6(a). The stator is found to operate at around 2.3 T as necessitated by CoFe lamination. Finally, the iron loss density of the benchmark

3
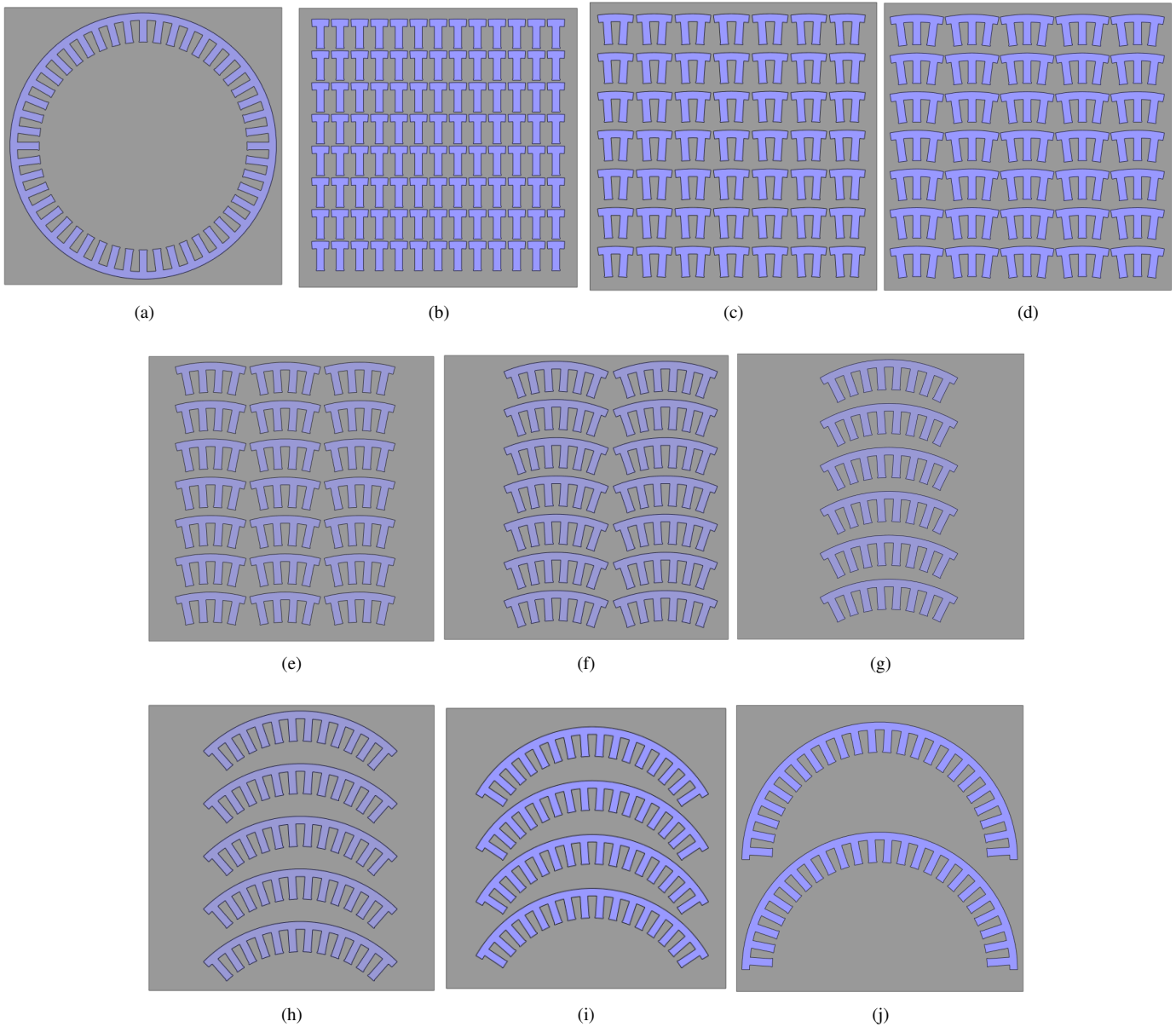
Figure 7: (a) No segmentation (b) single-tooth segmentation (c) two-teeth segmentation (d) three-teeth segmentation (e) four-teeth segmentation (f) six-teeth segmentation (g) eight-teeth segmentation (h) twelve-teeth segmentation (i) sixteen-teeth segmentation (j) twenty-four-teeth segmentation

Halbach PMSM is shown in Figure 6(b)

Overview of Stator Segmentation

The impact of stator segmentation on the utilization of stator lamination is studied in this section. The benchmark PMSM comprises of 48 slots. Tooth segmentation at the tooth-yoke interface is realizable for all stator designs and independent of the number of stator slots. On the other hand, the possible combination into which the stator can be segmented at the core is influenced by the total number of stator slots. This is dictated by the divisors of the number of stator slots. The divisors of 48 are 1, 2, 3, 4, 6, 8, 12, 16, 24 and 48. These divisors indicate the possible number of teeths in a segment. 48 represents the conventional single piece stator as shown in Figure 7(a). The segments corresponding to all other divisors are shown in Figures 7(b) - 7(j).

Maximizing the utilization of stator lamination is the main aim of this analysis. Therefore, it is essential to identify the utilization of stator lamination in all configurations. The size of lamination required for this analysis is selected based on the conventional single-piece design without stator segmentation. A square lamination with edge length greater than the stator outer diameter of the propulsion machine is necessary for single-piece cutting. Consequently, a square lamination with edge length 20 mm more than the stator outer diameter is considered for this analysis. 20 mm is provided to hold the lamination during the cutting process.

The total number of segments which can be cut from the selected square lamination varies for all the configurations as shown in Figure 7 and listed in Table 3. The number of complete stator lamination which can be assembled using the segments cut from the selected square lamination also various for all the configurations. The number of segments required for one complete stator lamination is given in Table 3. Based on the values given in Table 3, 2 complete set of stator laminations are obtainable from the selected square lamination for single-tooth, two-teeth and three-teeth segmentations. In contrast, only one complete set of stator lamination is obtainable using twelve-teeth, sixteen-teeth and twenty-four-teeth configurations. Therefore, it is essential to define a factor to compare all types of stator segmentation. Consequently,

4

Table 3: Utilization factor realizable with different types of stator segmentation

Type of stator segmentation	Number of segments obtainable from selected square lamination	Number of segments required for one complete stator lamination
No segmentation	1	1
Single-tooth	104	48
Two-teeth	49	24
Three-teeth	35	16
Four-teeth	21	12
Six-teeth	14	8
Eight-teeth	6	6
Twelve-teeth	5	4
Sixteen-teeth	4	3
Twenty-four-teeth	2	2

Table 4: Utilization factor realizable with different types of stator segmentation

Type of stator segmentation	Utilization factor
No segmentation	0.18
Single-tooth	0.39
Two-teeth	0.37
Three-teeth	0.39
Four-teeth	0.31
Six-teeth	0.31
Eight-teeth	0.18
Twelve-teeth	0.22
Sixteen-teeth	0.24
Twenty-four-teeth	0.18

utilization factor as defined in (1) is used to identify the maximum achievable stator lamination from the selected square lamination.

$$\text{Utilization factor} = \frac{\text{Achievable area of stator lamination}}{\text{Area of selected square lamination}} \quad (1)$$

The utilization factor for all configurations are calculated using (1) and listed in Table 4. The utilization factor is high for single-tooth, two-teeth, three-teeth, four-teeth and six-teeth configurations. The utilization factor is same for both four-teeth and six-teeth configurations. Segmentation into six-teeth will result in lesser number of total parts to be assembled in comparison to four-teeth configuration. This reduces complexity of the assembly process and thereby, its associated savings. Considering all these, single-tooth, two-teeth three-teeth, and six-teeth are the core segmented configurations which are selected for further analysis.

Impact of Stator Segmentation

Both tooth and core segmented topologies are studied to understand the impact of resulting airgap on the performance parameters like average torque, torque ripple and iron loss. Dovetail joint is selected at the interface of two segments. Two tooth-segmented and four core-segmented topologies as shown in Figure 8 are analyzed in this section. The size of the dovetail is found to be the only degree of freedom in tooth-segmented topologies. Consequently, a tooth segmented topology with big dove tail joint (Tooth 1) and another with small dovetail joint (Tooth 2) as shown in Figures 8(a) and 8(b) respectively are selected for analysis. In case of core segmented topologies, single-tooth, two-teeth, three-teeth and six-teeth as identified in the previous section
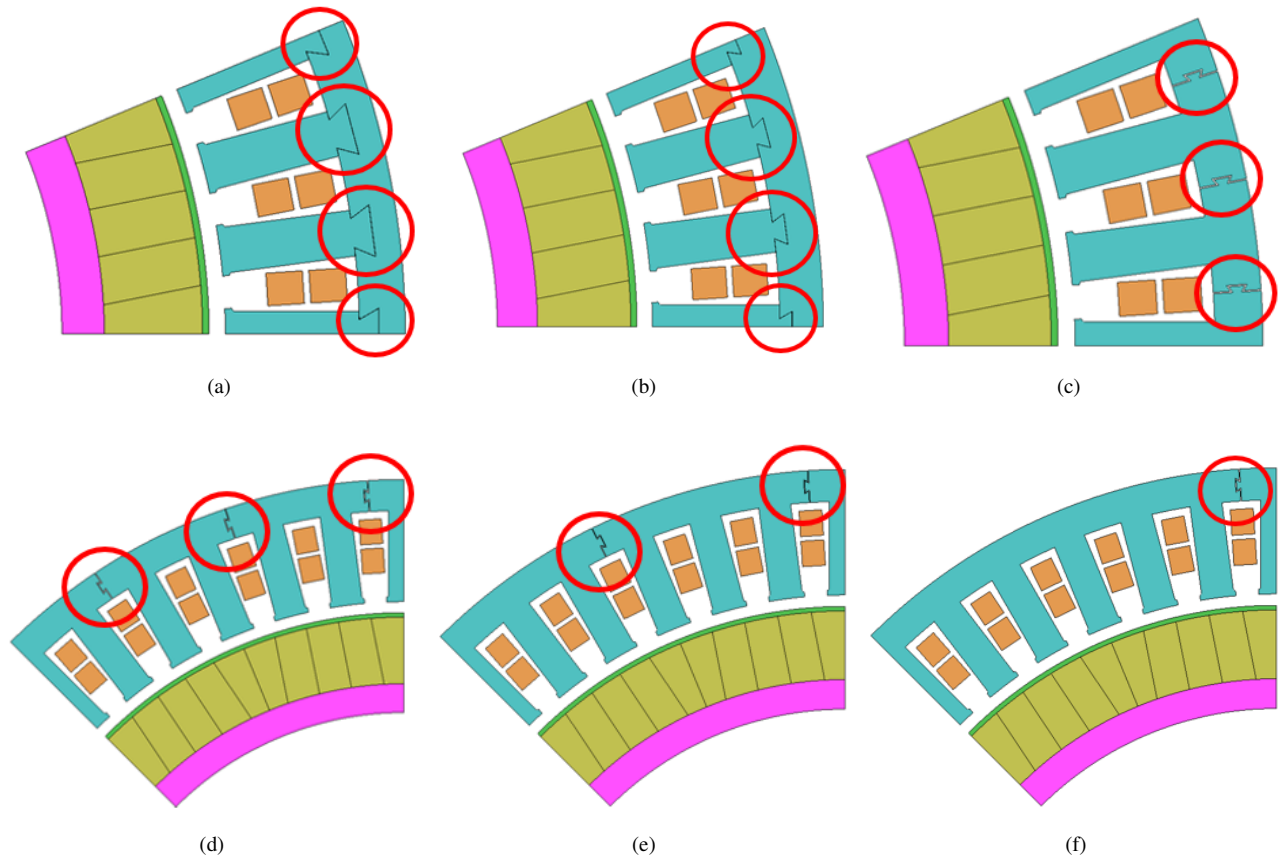
Figure 8: Topologies showing (a) tooth-segmentation with big dovetail joint (b) tooth-segmentation with small dovetail joint (c) single-tooth segmentation (d) two-teeth segmentation (e) three-teeth segmentation (f) six-teeth segmentation

(a)

(b)
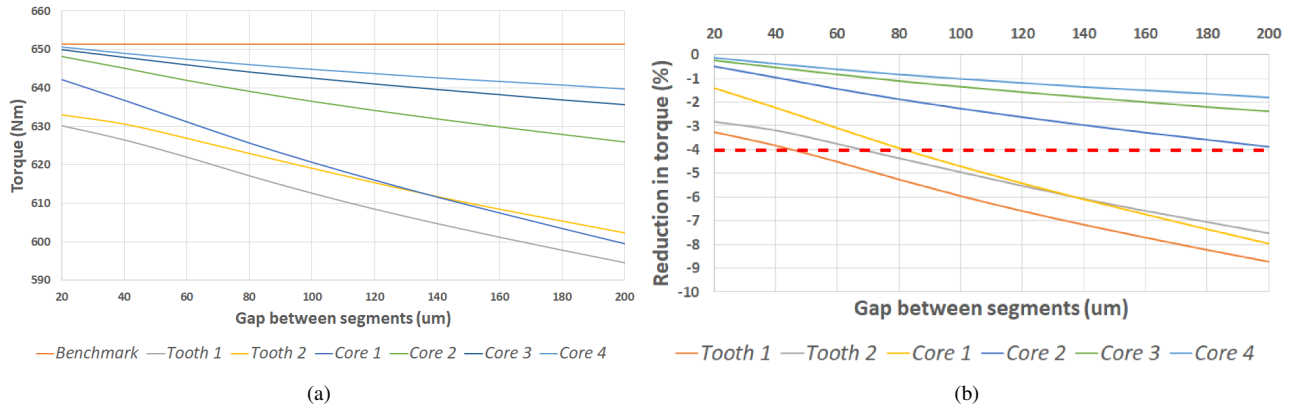
Figure 9: Simulation result at rated operating conditions with different airgap between segments for all segmented configurations showing (a) average torque (b) reduction in average torque compared to benchmark

(a)

(b)
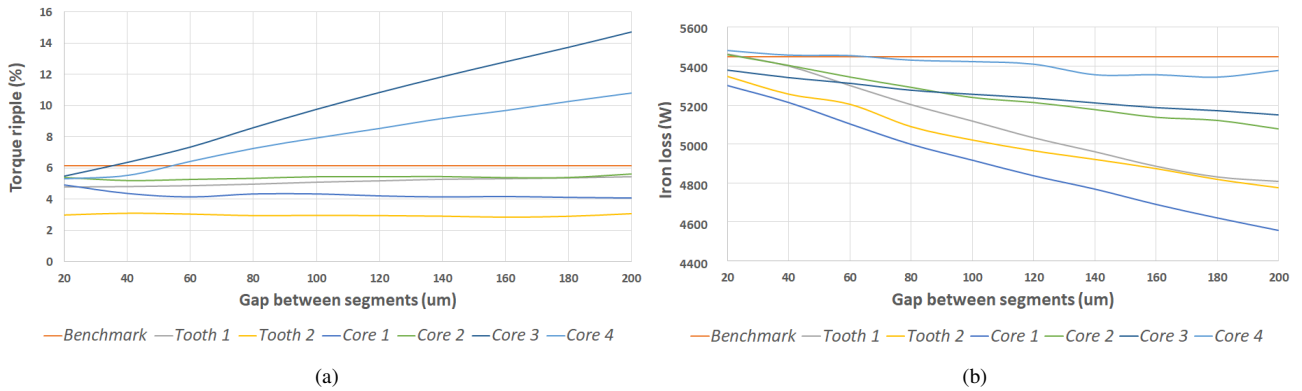
Figure 10: Simulation result at rated operating conditions with different airgap between segments for all segmented configurations showing variation compared to benchmark model for (a) torque ripple (b) iron loss

are subjected to further study.

The interface between two segments or dovetail joint is highlighted using a red circle for all the configurations in Figure 8. Symmetry favours simulation of a single pole for tooth-segmented and single-tooth core segmented topologies. However, simulation over a pole pair is required in case of two-teeth, three-teeth and six-teeth core segmented configurations as shown in Figure 8. Stator segmentation enables increased utilization of lamination. On the other hand, the resulting airgap at the interface deteriorates the electromagnetic performance. Therefore, a tight tolerance is required on the segmented parts to reduce the resulting airgap and thereby curtail its adverse effect on the electromagnetic performance. In contrast, a tight tolerance adds significantly to the cost of manufacturing and nullifies the savings obtained from segmentation. Consequently, it is required to weigh all the configurations based on two parameters, namely, utilization of lamination and minimum required tolerance to prevent adverse degradation of electromagnetic performance.

The airgap between two segments is highly not uniform in nature [12]. The current study performed in this paper is focused on the overall performance degradation rather than localized impact. Therefore, the resulting airgap is modelled as an average uniform value. A range of 20 μm to 200 μm in steps of 20 μm is selected for the resulting airgap thickness to analyze the impact of stator segmentation. 20 μm requires the best of cutting methods while 200 μm highly relaxes the manufacturing related requirements.

The reduction in average torque with an increase in airgap between segments for all the configurations is shown in Figure 9(a). Tooth 1 with bigger dovetail is found to have a higher degradation in aver-

age torque compared to Tooth 2 with smaller dovetail joints. Core 1, Core 2, Core 3 and Core 4 correspond to single-tooth, two-teeth, three-teeth and six-teeth core segmented configurations. The total number of airgap between segments in one-tooth, two-teeth, three-teeth and six-teeth configurations are 48, 24, 12 and 8 respectively. The average torque is found to increase in the order Core 1 < Core 2 < Core 3 < Core 4. This is inversely proportional to the total number of airgap between segments i.e., single-tooth with the most number of airgap between segments exhibits the highest reduction in average torque while six-teeth segmentation has the least reduction. The percentage reduction in average torque for all the stator segmented configurations in comparison to benchmark single-piece stator is shown in Figure 9(b). In can also be observed that the reduction in average torque is more in case of tooth segmented configurations. This identifies core segmentation as the better method for stator segmentation.

The maximum allowable airgap between stator segments to limit the degradation in average torque to 4% is obtained for all the configurations from Figure 9(b) and given in Table 5. It can be observed that a tighter tolerance is required with an increase in the number of stator segments and vice versa. Based on this, two-teeth segmentation is found to be beneficial in terms of utilization of lamination as well as reduced tolerance requirement.

The impact of stator segmentation on torque ripple and iron loss are shown in Figures 10(a) and 10(b) respectively. Torque ripple is found to be nearly constant between 20 μm to 200 μm for Tooth 1, Tooth 2, Core 1 and Core 2. On the other hand, the torque ripple is found to increase with the airgap thickness in case of three-teeth and six-teeth configurations. Therefore, configurations with more number of stator segments are preferred to have reduced effect on torque ripple. Finally,

6

Table 5: Airgap allowed between stator segments to limit the degradation in average torque to 4%

Type of stator segmentation	Allowable airgap between segments (μm)
Tooth 1	45
Tooth 1	70
Single-tooth	80
Two-teeth	200
Three-teeth	> 200
Six-teeth	> 200

the iron loss decreases with an increase in airgap between segments for all the configurations. This is due to reduced flux resulting from increased airgap between segments. The rate of decrease in more pronounced in configurations with more number of stator segments.

Conclusion

Electric machines offering a high power density are required for aerospace applications. Expensive CoFe lamination with a high saturation flux density is one of the key component which is required to realize these power density targets. The conventional method of single-piece stator fabrication results in enormous waste of expensive lamination in case of aerospace propulsion machines having a big bore diameter. Stator segmentation is identified as an appropriate method to reduce the wastage and cost associated with lamination. Consequently, in this paper, stator segmentation is analyzed on a 1.35 MW, 16-pole 48-slot propulsion machine. The impact of manufacturing is accounted by controlling the resulting airgap between the segmented structures. Electromagnetic performance for various segmented topologies are compared in terms of torque, torque ripple, and iron loss. The major outcomes of this work are as follows:

- In case of core segmented topologies, the utilization factor is more for the configurations having smaller segments in comparison to bigger segments.

- The reduction in average torque is more in case of tooth segmented configurations. This identifies core segmentation as the better method for stator segmentation.

- Tooth 1 with bigger dovetail is found to have a higher degradation in average torque compared to Tooth 2 with smaller dovetail joints. Single-tooth with the most number of airgap between segments exhibits the highest reduction in average torque while six-teeth segmentation has the least reduction.

- Configurations with more number of stator segments are preferred to have reduced effect on torque ripple.

- The iron loss decreases with an increase in airgap between segments for all the stator segmented configurations. The rate of decrease in more pronounced in configurations with more number of stator segments.

Contact Information

R. M. Ram Kumar
Ram.Ramanathan@nottingham.ac.uk

Acknowledgments

References

1. D. Golovanov, D. Gerada, G. Sala, M. Degano, A. Trentin, P. H. Connor, Z. Xu, A. L. Rocca, A. Galassini, L. Tarisciotti, C. N. Eastwick, S. J. Pickering, P. Wheeler, J. Clare, M. Filipenko, and C. Gerada, "4-mw class high-power-density generator for future hybrid-electric aircraft," *IEEE Transactions on Transportation Electrification*, vol. 7, no. 4, pp. 2952–2964, 2021.

2. T. Austin-Morgan, "Hybrid-electric propulsion could help cut emissions, noise and fuel use for commercial aircraft," 02 2018.

3. C. Gerada, M. Galea, and A. Kladas, "Electrical machines for aerospace applications," in *2015 IEEE Workshop on Electrical Machines Design, Control and Diagnosis (WEMDCD)*, pp. 79–84, 2015.

4. A. Boglietti, A. Cavagnino, A. Tenconi, S. Vaschetto, and P. di Torino, "The safety critical electric machines and drives in the more electric aircraft: A survey," in *2009 35th Annual Conference of IEEE Industrial Electronics*, pp. 2587–2594, 2009.

5. A. El-Refaie and M. Osama, "High specific power electrical machines: A system perspective," *CES Transactions on Electrical Machines and Systems*, vol. 3, no. 1, pp. 88–93, 2019.

6. B. Wu, Y. Li, D. Zhu, and Y. Qin, "Optimal design of a high power density pm motor with discrete halbach array and concentrated windings," *2011 International Conference on Electrical Machines and Systems*, pp. 1–5, 2011.

7. M. Cossale, A. Krings, J. Soulard, A. Boglietti, and A. Cavagnino, "Practical investigations on cobalt-iron laminations for electrical machines," in *2014 International Conference on Electrical Machines (ICEM)*, pp. 1390–1395, 2014.

8. M. Galea, Z. Xu, C. Tighe, T. Hamiti, C. Gerada, and S. Pickering, "Development of an aircraft wheel actuator for green taxiing," in *2014 International Conference on Electrical Machines (ICEM)*, pp. 2492–2498, 2014.

9. M. Centner and U. Schafer, "Optimized design of high-speed induction motors in respect of the electrical steel grade," *IEEE Transactions on Industrial Electronics*, vol. 57, no. 1, pp. 288–295, 2010.

10. A. D. Anderson, N. J. Renner, Y. Wang, S. Agrawal, S. Sirimanna, D. Lee, A. Banerjee, K. Haran, M. J. Starr, and J. L. Felder, "System weight comparison of electric machine topologies for electric aircraft propulsion," in *2018 AIAA/IEEE Electric Aircraft Technologies Symposium (EATS)*, pp. 1–16, 2018.

11. J. Rens, S. Jacobs, L. Vandenbossche, and E. Attrazic, "Effect of stator segmentation and manufacturing degradation on the performance of ipm machines, using icare® electrical steels," *World Electric Vehicle Journal*, vol. 8, no. 2, pp. 450–460, 2016.

12. Z. Q. Zhu, Z. Azar, and G. Ombach, "Influence of additional air gaps between stator segments on cogging torque of permanent-magnet machines having modular stators," *IEEE Transactions on Magnetics*, vol. 48, no. 6, pp. 2049–2055, 2012.

13. J. Richnow, D. Gerling, and P. Stenzel, "Torque ripple reduction in permanent magnet synchronous machines with concentrated windings and pre-wound coils," in *2014 17th International Conference on Electrical Machines and Systems (ICEMS)*, pp. 2501–2507, 2014.

14. D. Golovanov, D. Gerada, G. Sala, M. Degano, A. Trentin, P. H. Connor, Z. Xu, A. L. Rocca, A. Galassini, L. Tarisciotti, C. N. Eastwick, S. J. Pickering, P. Wheeler, J. Clare, M. Filipenko, and C. Gerada, "4-mw class high-power-density generator for future hybrid-electric aircraft," *IEEE Transactions on Transportation Electrification*, vol. 7, no. 4, pp. 2952–2964, 2021.